Original Research

Phosphorylation status of human RNA-binding protein 8A in cells and its inhibitory regulation by Magoh

Yasuhito Ishigaki[1], Yuka Nakamura[1], Takanori Tatsuno[1], Shaofu Ma[1] and Naohisa Tomosugi[1,2]

[1]Medical Research Institute, Kanazawa Medical University, Uchinada, Kahoku, Ishikawa 920-0293, Japan; [2]Medical Care Proteomics Biotechnology Co., Ltd., Uchinada-machi, Kahoku 920-0293, Japan
Corresponding author: Yasuhito Ishigaki. Email: ishigaki@kanazawa-med.ac.jp

Abstract

The RNA-binding protein 8A (RBM8A)–mago-nashi homolog, proliferation-associated (Magoh) complex is a component of the exon junction complex (EJC) required for mRNA metabolism involving nonsense-mediated mRNA decay (NMD). RBM8A is a phosphorylated protein that plays some roles in NMD. However, the detailed status and mechanism of the phosphorylation of RBM8A is not completely understood. Therefore, in this study, we analyzed in detail RBM8A phosphorylation in human cells. Accordingly, analysis of the phosphorylation status of RBM8A protein in whole-cell lysates by using Phos-tag gels revealed that the majority of endogenous RBM8A was phosphorylated throughout the cell-cycle progression. Nuclear and cytoplasmic RBM8A and RBM8A in the EJC were also found to be mostly phosphorylated. We also screened the phosphorylated serine by mutational analysis using Phos-tag gels to reveal modifications of serine residues 166 and 168. A single substitution at position 168 that concomitantly abolished the phosphorylation of serine 166 suggested the priority of kinase reaction between these sites. Furthermore, analysis of the role of the binding protein Magoh in RBM8A phosphorylation revealed its inhibitory effect *in vitro* and *in vivo*. Thus, we conclude that almost all synthesized RBM8A proteins are rapidly phosphorylated in cells and that phosphorylation occurs before the complex formation with Magoh.

Keywords: mRNA, RBM8A(Y14), Magoh, phosphorylation, Phos-tag gel

***Experimental Biology and Medicine* 2015; 240: 438–445. DOI: 10.1177/1535370214556945**

Introduction

An exon junction complex (EJC) forms on each exon–exon junction of spliced mRNAs according to the splicing reaction. This complex is composed of eukaryotic initiation factor 4A-III (eIF4A3), cancer susceptibility candidate 3 (Casc3 or metastatic lymph node 51 [MLN51]), mago-nashi homolog, proliferation-associated (*Drosophila*) (Magoh), RNA-binding protein 8A (RBM8A or Y14), Upf3, and other proteins.[1,2] It has been proposed that the EJC is required for mRNA metabolism via mRNA export and the nonsense-mediated mRNA decay (NMD) pathway and that NMD-related factors assemble the decaying complex onto mRNA via the EJC.[3–5] Therefore, this complex is required for some part of the NMD reaction. After the first round of translation by the ribosome, the EJC is eliminated from the mRNA molecules and reused at the splicing site of the nuclei.[1,6]

RBM8A is a member of the RNA-binding motif protein family[7] that forms a tight heterodimer with Magoh,[8] and it is localized onto mRNA via complex formation with other proteins.[9,10] Recent studies revealed the contributions of the RBM8A–Magoh complex to the decapping and methylosome activity, which are believed to be independent of the function of the EJC on mRNA.[11,12]

RBM8A and Magoh can form a complex with the signal transducer and activator of transcription 3 (STAT3), which regulates the cytokine regulator pathway, and the novel function of the complex in the STAT3-mediated transcription has been reported.[13,14] Furthermore, RBM8A upregulates the tumor necrosis factor-alpha (TNF-α)-induced transcriptional activity of nuclear factor-kappa beta in STAT3-dependent and -independent manners.[15] Inaki *et al.*[16] revealed the contribution of Magoh to the regulation of cyclin-dependent kinase (Cdk) in a temperature-sensitive cell-cycle mutant experiment. Because Cdk is essential for mitosis progression, this finding strongly implies the contribution of Magoh to cell proliferation, independent of the formation of the EJC. Le Hir *et al.*[17] also demonstrated the association between RBM8A and Magoh and showed that the depletion of these proteins in *Drosophila* SL2 cells

resulted in impaired cell growth. Furthermore, Sudo *et al.*[18] obtained similar results after performing a loss-of-function screening of genes involved in apoptosis and growth in the human mesothelioma cell line. These authors demonstrated the role of *RBM8A*, in addition to that of *COPA*, in cell growth via gene-silencing experiments using an RNAi library. Recently, the novel function of Magoh in mouse neural stem cell division as well its contribution to efficient centrosome maturation in neural progenitor cells was proposed.[19] These results were confirmed in a human tumor cell line, and the contribution of Magoh to the G2/M phase progression has also been proposed.[20] Thus, RBM8A and Magoh are associated with centrosome maturation, and their deficiency results in G2/M accumulation, followed by cell apoptosis. Furthermore, we found that RBM8A localizes to the centrosome in human tumor cells and proposed a novel function for this association.[21]

The phenotypes expressed owing to RBM8A deficiency or Magoh deficiency are different between human and mice. The deletion of human chromosome 1q21.1 has been frequently found in thrombocytopenia-absent radius (TAR) syndrome patients, and *RBM8A* is mapped to this region. Albers *et al.*[22] reported that TAR syndrome is caused by the compound heterozygosity of a 1q21.1 deletion and rare single nucleotide polymorphisms in the *RBM8A* region. TAR syndrome patients do not share any common phenotypes with Magoh-deficient mice. Furthermore, Kataoka *et al.*[5] performed mutational analysis to demonstrate the independent shuttling of RBM8A between the nucleoplasm and the cytoplasm, and Togi *et al.*[15] discovered an independent role for RBM8A, in addition to complex formation with Magoh. Therefore, it is speculated that Magoh and RBM8A have independent functions in cells, in addition to their shared functions in mRNA metabolism.

Hsu *et al.*[23] reported the importance of RBM8A phosphorylation *in vitro* and *in vivo*, and identified the phosphorylation of the protein at serine residues 166 and 168.[23] Hsu *et al.*[23] also showed that SRPK1, which is a member of the SR protein kinase family, phosphorylated the RBM8A protein *in vitro*. These authors also performed immunoprecipitation (IP) experiments and discovered the modulating effect of phosphorylation. It was proposed that the formation of an mRNA–protein complex by RBM8A and Magoh was regulated by RBM8A phosphorylation. These authors proposed that RBM8A phosphorylation occurs to release the protein from the mRNA–protein complex in the cytoplasm after the first round of translation for NMD. In summary, they showed that the phosphorylation and dephosphorylation of RBM8A are important for NMD and processing body formation and proposed a novel model for RBM8A-mediated mRNA decapping and degradation.[11]

In this study, we focused on the status and mechanism of RBM8A phosphorylation. First, we analyzed the phosphorylation status of RBM8A by Phos-tag gel analysis, which enabled detection of phosphorylated proteins by western blotting and modified sodium dodecyl sulfate-polyacrylamide gel electrophoresis (SDS-PAGE). The majority of the endogenous cellular RBM8A was phosphorylated in cell lysates. The mutational and expression analyses revealed the occurrence of serine phosphorylation at positions 166 and 168, in accordance with the report of Hsu *et al.*,[23] and our experiments also revealed the priority of serine phosphorylation at position 168 in cells. In addition, we showed that Magoh binding has an inhibitory effect on RBM8A phosphorylation *in vitro*.

Materials and methods

Cell culture

HeLa cells were purchased from the RIKEN cell bank (RIKEN Bio Resource Center, Tsukuba, Japan) and maintained in Dulbecco's Modified Eagle's Medium (Sigma-Aldrich, St. Louis, MO, USA) supplemented with 10% fetal bovine serum (Sigma-Aldrich) and antibiotics (a mixture of penicillin and streptomycin; Wako Pure Chemical Industries Ltd, Osaka, Japan).

Preparation of cell lysates

The cells were harvested using a lysis buffer containing PhosSTOP Phosphatase Inhibitor Cocktail (Roche Diagnostics Ltd, Basel, Switzerland). Phosphatase treatments were performed by adding lambda PPase (final concentration, 5 U/μL; New England Biolabs, Ipswich, MA, USA) to the lysis buffer, followed by incubation for 30 min at 37°C. After treatment, the samples were used for Phos-tag gel analysis.

SDS-PAGE, Phos-tag gel separation, and western blotting

Phos-tag gels (12.5%; Wako Pure Chemical Industries Ltd) enabled the separation of phosphorylated polypeptides from their unphosphorylated counterparts in SDS-PAGE.[24,25] The gel was transferred onto a nylon membrane, standard immunoblotting was performed, and phosphorylation was detected based on the upward shifting of bands to a greater molecular weight. Conventional SDS-PAGE was performed by using the SuperSep Gel (12.5%; Wako Pure Chemical Industries Ltd). A Wide-view Prestained Protein Size Marker III (Wako Pure Chemical Industries Ltd) was used to determine the molecular weight of proteins in gels. The detailed method used for western blotting was as described in our previous study.[26] Anti-RBM8A antibody (Sigma-Aldrich) and rabbit antiserum prepared in our laboratory was used against the N-terminal region of RBM8A protein. HRP-conjugated Flag or Myc tag-specific antibodies were purchased from the Medical and Biological Laboratories, Co., Ltd (Nagoya, Japan) and affinity purified rabbit polyclonal anticancer susceptibility candidate 3 (Casc3) antibody was obtained from the Bethyl Laboratories Inc. (Montgomery, TX, USA).

Gene silencing using siRNA

The depletion of the RBM8A protein by gene silencing was performed as previously described.[20] In brief, *RBM8A* was silenced by using the Stealth Select RNAi™ siRNAs (HSS115053: shown in ''#2,'' HSS115054: shown in ''#3''), and Lipofectamine RNAiMAX (Invitrogen, Life

Technologies Corp.) was used to transfect the siRNAs. Two double-stranded molecules of the Stealth RNAi Negative Control Kit, MI(M) were used as negative controls.

Double thymidine blockage and release

Double thymidine blockage and release was performed as detailed in our previous study.[20] Briefly, the cell-cycle progression was blocked in HeLa cells via two incubations with 2.5 mM thymidine (Sigma-Aldrich) for 24 h. The cells were released from the G1/S phase, and the cell population was analyzed by flow cytometry at different incubation time periods.

IP

One day after seeding of the cells, knockdown of RBM8A was performed with siRNA (#2) and control (M) by using the RNAiMAX (Invitrogen). After 48 h of further incubation, the cells were scraped from the dish, transferred to a test tube, and centrifuged. The cell pellet was resuspended in IP buffer (20 mM Tris; pH 7.9, 300 mM NaCl, and 0.5% Igepal), lysed by sonication, and the supernatant was transferred into a fresh tube. The antibody was added to the supernatant. After incubation, protein G-conjugated agarose (Invitrogen) was added to the tube and mixed gently by a rotator. After washing with IP buffer, the residual buffer was removed and the sample buffer was added, followed by denaturation. The supernatant was collected in a test tube and immediately placed on an ice bath for western blotting.

Preparation of nuclear and cytoplasm extracts

Cells were seeded in a 10-cm cell culture dish and, just before confluence was reached, Buffer A (10 mM N-[2-Hydroxyethyl]piperazine-N′-[2-ethanesulfonic acid] [HEPES], 10 mM KCl, 0.1 mM ethylenediaminetetraacetic acid [EDTA], 1 mM dithiothreitol [DTT], 0.5% Igepal, and protease inhibitors) was added to the cells, and the dish was incubated at room temperature, following which the cells were scraped from the dish and the lysate was collected into a test tube. The test tube was then placed on an ice bath and the content was mixed by up and down by pipetting several times, followed by centrifugation. The supernatant was collected as extracts of the cytoplasm; Buffer B (20 mM HEPES, 400 mM NaCl, 1 mM EDTA, 20% glycerol, 1 mM DTT, and protease inhibitor) was added to the pellet and resuspended by pipetting up and down several times. The sample was then centrifuged and the supernatant was collected as the extract of nucleoplasm. To remove salts from the lysate for Phos-tag gel analysis, nuclear and cytoplasm extracts were exchanged with Buffer C (25 mM HEPES, 250 mM NaCl) by using the Amicon Ultra-0.5 Centrifugal Filter (Millipore, Corp., Billerica, MA, USA). Fractionation was confirmed by western blotting with anti-lamin A/C and anti-caspase-3 antibodies (Cell Signaling Technology, Inc., Danvers, MA, USA).

Plasmids and transfection

Original plasmids that can express Myc-tagged human RBM8A (EX-L0116-M09) or Flag-tagged Magoh (EX-I0115) were purchased from GeneCopoeia, Inc. (Rockville, MD, USA). The sequence was mutated by using the QuikChange Lightning Site-Directed Mutagenesis Kit (Agilent Technologies Inc., Santa Clara, CA, USA). The mutated sequences were confirmed by direct sequencing. Serine residues 42, 46, 56, 166, and 168 were replaced with alanine residues. The corresponding plasmids were named S42A, S46A, S56A, S166A, and S168A, respectively. In addition, a double mutant with S166A and S168A substitutions and a triple mutant with S42A, S46A, and S56A substitutions were produced. A plasmid containing all mutations (All-SA) was also constructed. For transfection of expression vectors, 80,000 HeLa cells were inoculated into 12-well plates (TPP Techno Plastic Products AG, Trasadingen, Switzerland) a day before the experiment. The plasmids were purified by using the Miniprep Kit (Qiagen, Hilden, Germany) and transfected by using the Effectene and Lipofectamine Transfection Kit (Qiagen), according to the manufacturer's protocol. One day after the transfection experiment, the cell lysates were prepared and analyzed.[26]

Recombinant proteins and *in vitro* kinase assay

His-tagged recombinant human RBM8A (Abcam PLC., Cambridge, UK), Magoh (Abcam PLC), and SRPK1 (Invitrogen) proteins were used in this study. Kinase buffer containing 100 mM Tris–HCl, 20 mM $MgCl_2$, 2 mM DTT, and 1.6 mM adenosine triphosphate (ATP) was used. To detect RBM8A phosphorylation by SRPK1, 30 ng of each protein was mixed in the kinase buffer with or without ATP and incubated for 30 min at 30°C. For analysis of inhibition by Magoh, RBM8A and Magoh were incubated for 30 min to form a complex, SRPK1 was subsequently added to the mixture, followed by incubation for 60 min at 30°C. The samples were denatured and separated on a Phos-tag gel, and RBM8A was detected using a mouse anti-RBM8A antibody (Sigma-Aldrich) or an anti-His-tag antibody directly conjugated to horseradish peroxidase (Medical & Biological Laboratories Co., Ltd).

Statistical analysis

To compare the average differences among the groups, Steel's test was performed. Student's *t*-test was performed for comparison of the average values between the two groups.

Results

The majority of RBM8A in the total cell lysate was found to be phosphorylated

HeLa cell lysates, prepared in lysis buffer and separated on a Phos-tag gel, were blotted using an anti-RBM8A antibody (Figure 1(a)). Phos-tag gels allow clear visualization of the fraction of phosphorylated proteins against the unphosphorylated counterpart because the proteins yield a large difference in migration. As indicated by the arrows in Figure 1(a), the position of the detected signal was completely different from that of the normal SDS-PAGE signal. In addition, we performed knockdown experiments to confirm the origin of bands. Both of the specific bands

were detected at approximately 20 kDa in the normal gel, and the shifted band detected in the Phos-tag gel disappeared after RBM8A knockdown. To test whether this band shift was caused by phosphorylation, the lysate was treated with phosphatase (lambda PPase) and then separated on a Phos-tag gel (Figure 1(b)). Almost all bands, including those showing specific and nonspecific signals, appeared at a higher molecular weight in the absence of PPase, whereas some bands appeared at approximately 20 kDa in the presence of PPase. Taken together, we conclude that the band shift observed in the Phos-tag gel was caused by the phosphorylation of the RBM8A protein. The majority of RBM8A bands shifted to a higher molecular weight in the Phos-tag gel, indicating that the majority of RBM8A is phosphorylated in cells.

Because our previous study suggested the contribution of RBM8A to the cell-cycle progression,[20] we analyzed the phosphorylation status of the protein at various cell-cycle stages. We then prepared the cells in the G1/S, S, and G2/M phases by releasing them from a double thymidine blockage (supplementary Figure 1). The polypeptides separated on gels were transferred onto a nylon membrane and blotted using a mouse anti-RBM8A antibody (Figure 2). The band size difference observed between the normal and Phos-tag gel was caused by the phosphorylation of target polypeptides, as shown in Figure 1. Band shifts were observed for all bands in all cell-cycle phases as well as in growing cells. Therefore, we concluded that the majority of RBM8A was phosphorylated in a stable manner throughout the cell cycle.

To investigate the dependency of cell location, we fractionated the cell lysate to nuclear and cytoplasmic fractions (Figure 3). Successful fractionation was confirmed by the detection of lamin A/C (nuclear marker) and caspase-3 (cytoplasmic marker) in the fractions.[27] The specificity of the band was examined by knockdown of RBM8A, and the band intensity reduced in the knockdown cells. Based on bands from lamin A/C and caspase-3, our fractionation was also successful, and RBM8A protein was detected in both of them. The band shift in the Phos-tag gel was observed in all lysate samples. We conclude that almost all of the RBM8A proteins are phosphorylated in both the nucleoplasm and cytoplasm.

Furthermore, to analyze the phosphorylation status of RBM8A in the EJC, we immunopurified the complex with anti-Casc3 antibody and separated it on normal and Phos-tag gels. Bands were detected by western blotting. The majority of immunopurified RBM8A and Casc3-bound RBM8A bands shifted in the Phos-tag gels (Figure 4). Therefore, we concluded that almost all RBM8A proteins in the EJC are also phosphorylated.

Determination of phosphorylated serine residues in the RBM8A polypeptide

To determine the phosphorylation sites of RBM8A, we prepared an expression vector containing Myc-tagged RBM8A with various serine-to-alanine substitutions based on an

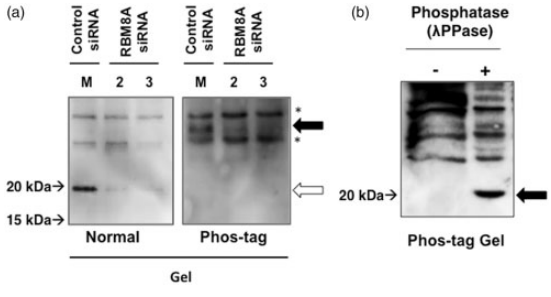

Figure 1 Phos-tag gel analysis of the RNA-binding protein 8A (RBM8A) in cell lysates. (a) The cells were transfected with control (M) and anti-RBM8A siRNA (lanes 2 and 3), and the cell lysates were collected. The samples were concomitantly separated on normal sodium dodecyl sulfate (SDS)-polyacrylamide gel (PAGE) or Phos-tag gel and transferred onto a nylon membrane. The membrane was blotted using an anti-RBM8A antibody and a horseradish peroxidase (HRP)-conjugated secondary antibody. (b) The cell lysates were treated with lambda PPase phosphatase and then separated on a Phos-tag gel. The membrane was blotted using an anti-RBM8A antibody. The black arrow indicates dephosphorylated RBM8A. In both the panels, the white arrow indicates the position of the RBM8A polypeptide in the normal gel (approximately 20 kDa), and the black arrow indicates the RBM8A protein in the Phos-tag gel. The asterisk (*) indicates a nonspecific signal

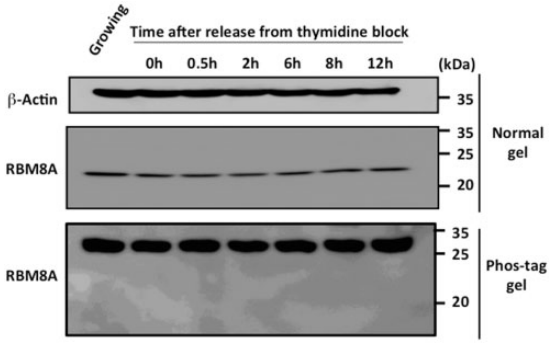

Figure 2 Phosphorylation of RBM8A at various cell-cycle phases. The samples were extracted from the growing and released cells at the G1/S stage by blocking. The cells were analyzed at 0, 0.5, 2, 6, 8, and 12 h after release. Flow cytometry analysis at each time point is shown in supplementary Figure 1, and the cells passed through the G1/S, S, and G2/M phases. The cell lysates were separated on normal SDS-PAGE and Phos-tag gels. After transfer onto a nylon membrane, the membrane was probed using an anti-RBM8A antibody. The positions of 20-, 25-, and 35-kDa bands are shown

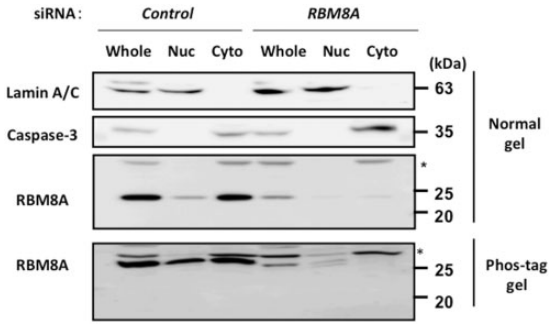

Figure 3 Phosphorylation of RBM8A in the cytoplasmic and nucleoplasmic fractions. The cells were fractionated and each fraction was separated on normal and Phos-tag gels. After transfer onto a membrane, western blotting was performed. Lamin A/C and Caspase-3 were used as markers of nucleoplasmic (Nuc) and cytoplasmic (Cyto) fractions. The knockdown lysate was also analyzed to detect specific bands

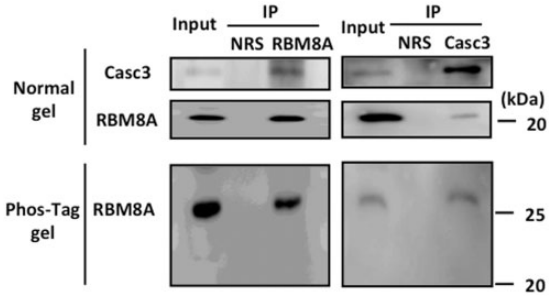

Figure 4 Phosphorylation of RBM8A in the EJC. RBM8A or Casc3 was immunopurified and analyzed in normal and Phos-tag gels. Input is the whole-cell lysate, and NRS indicates the control normal rabbit serum used in immunoprecipitation (IP). Immunopurified proteins were detected by western blotting

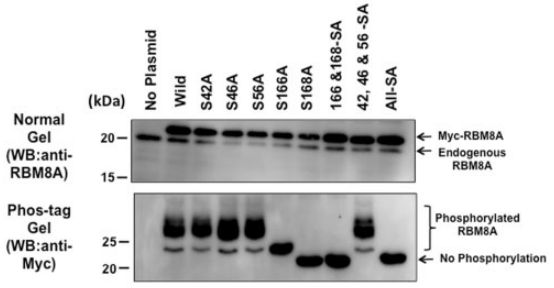

Figure 5 Determination of phosphorylated serine residues by Phos-tag gel analysis. Myc-tagged RBM8A expression vectors were transfected into HeLa cells, and cell lysates were separated on a Phos-tag gel. Serine residues 42, 46, and 56 are located on the N-terminal (N) side, and both the serine residues 166 and 168 are located at the C-terminal side (C) of the RNA-binding motif of RBM8A. Single or multiple serine-to-alanine substitutions were introduced. C-SA contained both the 166-SA and 168-SA mutations, and N-SA contained the 42, 46, and 56 triple mutations. All-SA had all the mutations (substitutions at positions 42, 46, 56, 166, and 168)

available database.[28–30] Plasmids containing single and multiple substitutions were developed. Phos-tag gels are extremely useful for the determination of the phosphorylation sites of various proteins.[31] Moreover, the combination of amino acid substitution and Phos-tag gel analysis enabled the determination of the phosphorylation sites.[32] The details of the mutant RBM8A clones are described in the legend of Figure 5, and the representative result is shown in Figure 5. Hsu *et al.*[23] reported that serine residues 166 and 168 of RBM8A are phosphorylated. Therefore, we reconfirmed their results by Phos-tag gel analysis. The plasmid vectors were transfected into HeLa cells and the cell lysates were prepared. The samples obtained were separated on a Phos-tag gel and detected using an anti-Myc-tag antibody. The main band of the wild-type RBM8A (Wild) appeared at approximately 30 kDa. In contrast, RBM8A with substitutions at five serine sites (All-SA) was detected at approximately 27 kDa. Therefore, the difference in separation was caused by the phosphorylation of Myc-tagged RBM8A. No significant difference was detected for proteins carrying a serine-to-alanine substitution at positions 42, 46, or 56; however, proteins with substitutions at residues 166 and 168 showed significant changes in migration. The position of the S168A band was identical to that of the All-SA substitution, suggesting that the mutant underwent similar phosphorylation. Compared with the S168A mutant, the S166A mutant yielded an additional band with slower migration. In summary, serine residues 166 and 168 of RBM8A were phosphorylated in HeLa cells and similar results were obtained in A549 cells (data not shown).

In vitro kinase assay and the inhibitory effect of Magoh

Hsu *et al.*[23] reported the phosphorylation of the RBM8A–Magoh heterodimer, as assessed in a kinase assay with SRPK1; however, the authors did not detect any effect of the Magoh protein on the kinase activity of SRPK1. Therefore, to determine the role of Magoh in phosphorylation, we performed an *in vitro* kinase assay with recombinant RBM8A, Magoh, and SRPK1. The polypeptides were mixed and incubated for 15 min at 30°C and separated on a Phos-tag gel, followed by western blotting (supplementary Figure 2). In the absence of ATP, no band shift to higher molecular weight region was detected, even with SRPK1 (lane 2 in the left panel); however, in the presence of ATP in the reaction mixture, significantly shifted bands were detected (lane 4 in the left panel). Therefore, Phos-tag gel analysis could detect *in vitro* RBM8A phosphorylation by SRPK1. In accordance with cell analysis in Figure 5, 166 and 168 SA mutation abolished the band shift in the Phos-tag gel (the right panel). Next, we mixed RBM8A and Magoh and incubated them for 30 min for complex formation. After incubation, SRPK1 was added to the complex for kinase reaction (Figure 6). The band shift in the Phos-tag gel disappeared according to the amount of Magoh. This result suggests that Magoh inhibits rather than accelerates the kinase activity of SRPK1 *in vitro*. To test this inhibitory effect *in vivo*, we co-transfected the Magoh and RBM8A expression vectors in HeLa cells. We observed an increase in the size of a band from exogenous RBM8A between that of the phosphorylated band from wild RBM8A and unphosphorylated band from 166/168SA mutant RBM8A (Figure 7, white arrow). Therefore, we speculate that Magoh affects RBM8A phosphorylation during the *in vivo* reaction and that the kinase reaction occurs rapidly in cells.

Discussion

One of our major findings was that the majority of RBM8A was phosphorylated in human cells. A similar result was obtained for the whole cell lysate (Figure 1), various cell-cycle steps (Figure 2), nuclear and cytoplasmic fractions (Figure 3), and the EJC (Figure 4). Immunostaining revealed that both RBM8A and Magoh localized to the nucleoplasm, indicating that the majority of RBM8A proteins in the nucleus were phosphorylated. It has been proposed that RBM8A phosphorylation contributes to its dissociation from the mRNA–protein complex after the first round of translation.[23] According to this model, only a limited fraction of cytoplasmic RBM8A should be phosphorylated. However, our results contradicted that of the aforementioned model. Thus, we proposed another possibility, i.e. rapid RBM8A phosphorylation occurs immediately after its biogenesis in the cytoplasm. Because the kinase reaction mediated by SRPK1 was inhibited by the association with

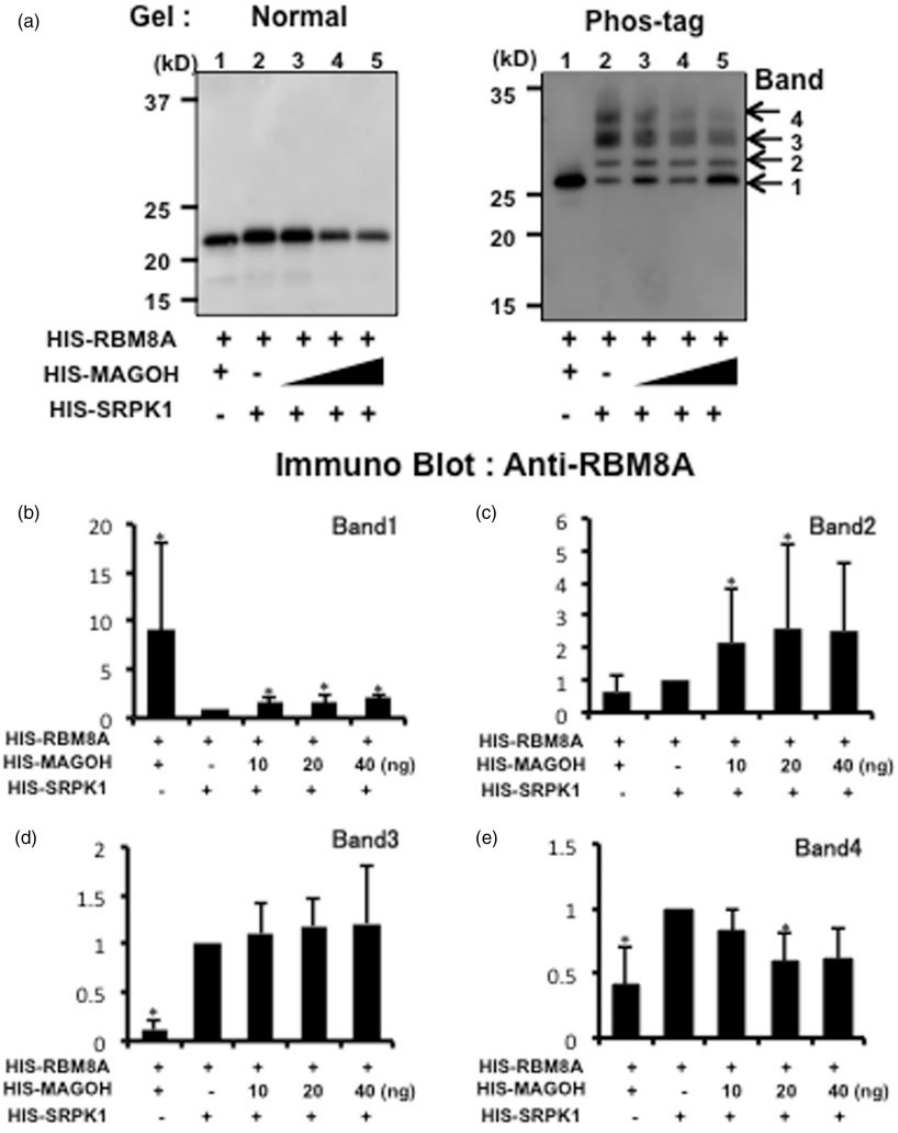

Figure 6 Effect of Magoh on the phosphorylation of RBM8A by SRPK1. Recombinant RBM8A and Magoh were mixed to form a complex. After complex formation, SRPK1 was added to the reaction mixture and incubated. After separation in the Phos-tag gel, the polypeptides were transferred onto a nylon membrane. RBM8A was detected using a mouse anti-RBM8A antibody. (a) Representative images of western blotting. (b–e) The intensity of four bands detected in the Phos-tag gel was measured, and the intensities are shown in the graph. Bar shows average of three independent experiments and bar means standard deviation. The asterisk (*) indicates $p < 0.05$

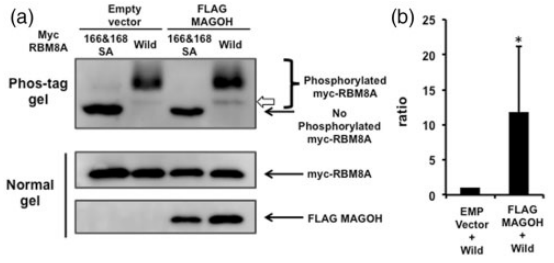

Figure 7 The effect of Magoh overexpression on RBM8A phosphorylation. The cells were co-transfected with Flag-tagged Magoh and Myc-tagged RBM8A, and the cell lysates were separated on normal and Phos-tag gels. For western blotting, anti-Flag antibody was used for the detection of Magoh, and anti-Myc antibody was used for the detection of RBM8A. 166&168 SA mutant was used as the negative control of phosphorylation. (a) Representative images. (b) The intensity of band indicated with the white arrow was measured, and the ratio of band intensity from wild RBM8A with or without Magoh overexpression is shown in the graph. Bar shows the average of three independent experiments and bar shows the standard deviation. The asterisk (*) indicates $p < 0.05$

Magoh (Figures 6 and 7), the RBM8A polypeptide produced should be phosphorylated before binding to Magoh. Therefore, RBM8A produced in the cytoplasm is probably phosphorylated, forms a complex with Magoh, and migrates to the nucleoplasm. In the nuclei, RBM8A may be dephosphorylated before splicing and assembled in the EJC on mRNA. As proposed by Chuang *et al.*,[11] after the first round of translation, RBM8A is dephosphorylated again and acts in decapping the decaying mRNA.[11]

In agreement with the findings reported by Hsu *et al.*,[23] our mutational analysis revealed that RBM8A phosphorylation occurs at serine residues 166 and 168. The serine-to-alanine substitution at either of the positions 166 or 168 or at both resulted in a band shift to a lower molecular weight as compared with that of the wild-type band (Figure 5). The bands corresponding to S42A, S46A, S56A, 42-SA, 46-SA, and 56-SA were found to be identical to those of the

wild-type protein, suggesting that these N-terminal serine residues are unphosphorylated. In contrast, the bands corresponding to S166A, S168A, 166-SA, 168-SA, and All-SA were different from those of the wild-type protein, with evident band shifts. The band shifts caused by the substitutions of the serine residues at positions 166 and 168 were different. The migration of S168A is identical to that of the negative controls such as All-SA and 42-SA, 46-SA, and 56-SA, whereas S166A yielded an additional band above the band of S168A. We speculate that S168A is unphosphorylated at the serine residues at positions 166 and 168, whereas serine 168 of the S166A mutant is phosphorylated. In addition, the analysis with SE mutants (substitution of serine with glutamic acid) showed results similar to those obtained with SA mutants (supplementary Figure 3). Therefore, we concluded that the phosphorylation reaction at serine 168 is required for phosphorylation at serine 166 rather than at serine 168. Although the present study did not identify the mechanism underlying this relationship, the relative priority can be attributed to structural characteristics or characterization of kinases.

The localization of RBM8A to the centrosome was described in our previous report.[21] To determine whether the phosphorylation of serine residue 166 or 168 is required for the localization of RBM8A to the centrosome, we immunostained the exogenously expressed Myc-RBM8A in the transfected cells. We successfully detected the localization of mutant RBM8A to gamma-tubulin-positive centrosomes (supplementary Figure 4). Thus, we conclude that the phosphorylation of these serine residues is not related to the localization of the centrosome.

An *in vitro* kinase reaction was performed to identify the role of Magoh in RBM8A phosphorylation. The three major band shifts observed in the Phos-tag gel were dependent on both ATP and the serine residues at positions 166 and 168 (supplementary Figure 2). The band shifts were not observed in the buffer devoid of ATP. In addition, both of mutation resulted in reduced band shift. Therefore, we concluded that these band shifts were caused by the phosphorylation of the RBM8A protein because in the present study, we demonstrated the inhibitory effect of Magoh on RBM8A phosphorylation (Figures 6 and 7). Magoh is a binding partner of RBM8A; however, its role in RBM8A phosphorylation remains unclear. Hsu *et al.*[23] used the RBM8A–Magoh heterodimer in an *in vitro* kinase assay, but did not detect the involvement of Magoh in this assay. We performed a kinase assay using RBM8A, Magoh, and SRPK1 kinase. After incubation of RBM8A with Magoh to form a heterodimer, we tested the kinase activity by adding SRPK1. RBM8A phosphorylation was reduced according to the amount of Magoh. Thus, we speculated that the synthesized RBM8A protein is phosphorylated before the formation of the heterodimer with Magoh because Magoh inhibited the SRPK1 reaction. Perhaps Magoh binds to phosphorylated RBM8A in the cells and is then transferred to the nucleoplasm to form the EJC on spliced mRNAs. Hsu *et al.*[23] and Chaung *et al.*[11] concluded that RBM8A phosphorylation occurs to facilitate dissociation from mRNP in the cytoplasm because compared with unphosphorylated RBM8A, phosphorylated RBM8A showed reduced affinity to NMD-related factors. The majority of RBM8A was phosphorylated in the cells (Figure 1); we believe that our conclusion is not in contrast with the experimental results of the previous studies. We also speculated that the majority of RBM8A in the nucleoplasm might be phosphorylated to avoid unnecessary complex formation with NMD factors. After NMD complex formation, when the ribosome encounters a premature termination codon, a phosphatase reaction takes places for association with decaying mRNA.[11]

In the present study, we revealed that the majority of RBM8A was phosphorylated in cells and that serine residues 166 and 168 were selectively phosphorylated, which indicates the priority of kinase reaction between these sites. RBM8A phosphorylation was inhibited by the Magoh protein *in vitro*. Because the phosphorylation and dephosphorylation mechanisms of the RBM8A protein may be complex, a more detailed analysis of this step-wise kinase reaction in the cells is required to completely understand RBM8A regulation.

Authors' contributions: All authors participated in the design and interpretation of the results, data analysis, and review of the manuscript. YI and NT conducted the experiments; YI, YN, TT, and SM performed the experiments; and YI and YN wrote the manuscript.

ACKNOWLEDGEMENTS

The present study was supported by grants from the Kanazawa Medical University (S2013-2, SR2012-02, C2014-3); Grants of Strategic Research Project [H2012-16 (S1201022)] from the Kanazawa Medical University, Ministry of Education, Culture, Sports, Science and Technology, Japan; and a Grant-in-Aid for Scientific Research in Japan (KAKENHI #25460376).

DECLARATION OF CONFLICTING INTERESTS

The authors declare the following conflict: Prof. Naohisa Tomosugi is the president of Medical Care Proteomics Biotechnology Co. Ltd. However, this association does not alter the authors' adherence to all the policies regarding sharing of data.

REFERENCES

1. Bono F, Gehring NH. Assembly, disassembly and recycling: the dynamics of exon junction complexes. *RNA Biol* 2011;**8**:24–29
2. Le Hir H, Séraphin B. EJCs at the heart of translational control. *Cell* 2008;**133**:213–6
3. Le Hir H, Gatfield D, Izaurralde E, Moore MJ. The exon-exon junction complex provides a binding platform for factors involved in mRNA export and nonsense-mediated mRNA decay. *Embo J* 2001;**20**:4987–97
4. Singh G, Lykke-Andersen J. New insights into the formation of active nonsense-mediated decay complexes. *Trends Biochem Sci* 2003;**28**:464–6
5. Kataoka N, Diem MD, Yoshida M, Hatai C, Dobashi I, Dreyfuss G, Hagiwara M, Ohno M. Specific Y14 domains mediate its nucleo-cytoplasmic shuttling and association with spliced mRNA. *Sci Rep* 2011;**1**:92
6. Gehring NH, Lamprinaki S, Kulozik AE, Hentze MW. Disassembly of exon junction complexes by PYM. *Cell* 2009;**137**:536–48

7. Salicioni AM, Xi M, Vanderveer LA, Balsara B, Testa JR, Dunbrack RL Jr, Godwin AK. Identification and structural analysis of human RBM8A and RBM8B: two highly conserved RNA-binding motif proteins that interact with OVCA1, a candidate tumor suppressor. *Genomics* 2000;**69**:54–62
8. Zhao XF, Colaizzo-Anas T, Nowak NJ, Shows TB, Elliott RW, Aplan PD. The mammalian homologue of mago nashi encodes a serum-inducible protein. *Genomics* 1998;**47**:319–22
9. Kataoka N, Diem MD, Kim VN, Yong J, Dreyfuss G. Magoh, a human homolog of Drosophila mago nashi protein, is a component of the splicing-dependent exon-exon junction complex. *Embo J* 2001;**20**:6424–33
10. Lau CK, Diem MD, Dreyfuss G, Van Duyne GD. Structure of the Y14-Magoh core of the exon junction complex. *Curr Biol* 2003;**13**:933–41
11. Chaung TW, Chaung WL, Lee KM, Tarn WY. The RNA-binding protein Y14 inhibits mRNA decapping and modulates processing body formation. *Mol Biol Cell* 2013;**24**:1–13
12. Chaung TW, Peng PJ, Tarn WY. The exon junction complex component Y14 modulates the activity of the methylosome in biogenesis of spliceosoimal small nuclear ribonucleoproteins. *J Biol Chem* 2011;**286**:8722–8
13. Muromoto R, Taira N, Ikeda O, Shiga K, Kamitani S, Togi S, Kawakami S, Sekine Y, Nanbo A, Oritani K, Matsuda T. The exon-junction complex proteins, Y14 and MAGOH regulate STAT3 activation. *Biochem Biophys Res Commun* 2009;**382**:63–68
14. Ohbayashi N, Taira N, Kawakami S, Togi S, Sato N, Ikeda O, Kamitani S, Muromoto R, Sekine Y, Matsuda T. An RNA biding protein, Y14 interacts with and modulates STAT3 activation. *Biochem Biophys Res Commun* 2008;**372**:475–9
15. Togi S, Shiga K, Muromoto R, Kato M, Somura Y, Sekine Y, kon S, Oritani K, Matsuda T. Y14 positively regulates TNF-α-induced NF-κB transcriptional activity via interacting RIP1 and TRADD beyond an exon junction complex protein. *J Immunol* 2013;**191**:1436–44
16. Inaki M, Kato D, Utsugi T, Onoda F, Hanaoka F, Murakami Y. Genetic analyses using a mouse cell cycle mutant identifies magoh as a novel gene involved in Cdk regulation. *Genes Cells* 2011;**16**:166–78
17. Le Hir H, Gatfield D, Braun IC, Forler D, Izaurralde E. The protein Mago provides a link between splicing and mRNA localization. *Embo Rep* 2001;**2**:1119–24
18. Sudo H, Tsuji AB, Sugyo A, Kohda M, Sogawa C, Yoshida C, Harada YN, Hino O, Saga T. Knockdown of COPA, identified by loss-of-function screen, induces apoptosis and suppresses tumor growth in mesothelioma mouse model. *Genomics* 2010;**95**:210–6
19. Silver DL, Watkins-Chow DE, Schreck KC, Pierfelice TJ, Larson DM, Burnetti AJ, Liaw HJ, Myung K, Walsh CA, Gaiano N, Pavan WJ. The exon junction complex component Magoh controls brain size by regulating neural stem cell division. *Nat Neurosci* 2010;**13**:551–8
20. Ishigaki Y, Nakamura Y, Tatsuno T, Hashimoto M, Shimasaki T, Iwabuchi K, Tomosugi N. Depletion of RNA-binding protein RBM8A (Y14) causes cell cycle deficiency and apoptosis in human cells. *Exp Biol Med* 2013;**238**:889–97
21. Ishigaki Y, Nakamura Y, Tatsuno T, Hashimoto M, Iwabuchi K, Tomosugi N. RNA binding protein RBM8A (Y14) and MAGOH localize to centrosome in human A549 cells. *Histochem Cell Biol* 2013;**141**:101–9
22. Albers CA, Paul DS, Schulze H, Freson K, Stephens JC, Smethurst PA, Jolley JD, Cvejic A, Kostadima M, Bertone P, Breuning MH, Debili N, Deloukas P, Favier R, Fiedler J, Hobbs CM, Huang N, Hurles ME, Kiddle G, Krapels I, Nurden P, Ruivenkamp CAL, Sambrook JG, Smith K, Stemple DL, Strauss G, Thys C, van Geet C, Newbury-Ecob R, Ouwehand WH, Ghevaert C. Compound inheritance of a low-frequency regulatory SNP and a rare null mutation in exon-junction complex subunit RBM8A causes TAR syndrome. *Nat Genet* 2012;**44**:435–9
23. Hsu laW, Hsu M, Li C, Chuang TW, Lin RI, Tarn WY. Phosphorylation of Y14 modulates its interaction with proteins involved in mRNA metabolism and influences its methylation. *J Biol Chem* 2005;**280**:34507–12
24. Kinoshita E, Kinoshita-Kikuta E, Koike T. Separation and detection of large phosphoproteins using Phos-tag SDS-PAGE. *Nat Protoc* 2009;**4**:1513–21
25. Kinoshita E, Kinoshita-Kikuta E, Takiyama K, Koike T. Phosphate-binding tag, a new tool to visualize phosphorylated proteins. *Mol Cell Proteomics* 2006;**5**:749–57
26. Maru S, Ishigaki Y, Shinohara N, Takata T, Tomosugi N, Nonomura K. Inhibition of mTORC2 but not mTORC1 up-regulates E-cadherin expression and inhibits cell motility by blocking HIF-2α expression in human renal cell carcinoma. *J Urol* 2013;**189**:1921–9
27. Zhao X, Nogawa A, Matsunaga T, Takegami T, Nakagawa H, Ishigaki Y. Proteasome inhibitors and knockdown of SMG1 cause accumulation of Upf1 and Upf2 in human cells. *Int J Oncol* 2014;**44**:222–8
28. Mahen R, Venkitaraman AR. Pattern formation in centrosome assembly. *Curr Opin Cell Biol* 2012;**24**:14–23
29. Bettencourt-Dias M, Glover DM. Centrosome biogenesis and function: centrosomics brings new understanding. *Nat Rev Mol Cell Biol* 2007;**8**:451–63
30. Ma HT, Poon RY. How protein kinases co-ordinate mitosis in animal cells. *Biochem J* 2011;**435**:17–31
31. Kinoshita-Kikuta E, Aoki Y, Kinoshita E, Koike T. Label-free kinase profiling using phosphate affinity polyacrylamide gel electrophoresis. *Mol Cell Proteomics* 2007;**6**:356–66
32. Hosokawa T, Saito T, Asada A, Fukunaga K, Hisanaga S. Quantitative measurement of in vivo phosphorylation states of Cdk5 activator p35 by Phos-tag SDS-PAGE. *Mol Cell Proteomics* 2010;**9**:1133–43

(Received January 27, 2014, Accepted September 11, 2014)